Direct observation of a time-delayed intermediate state generated via exciton-exciton annihilation in polyfluorene

Qing-Hua Xu, Daniel Moses,* and Alan J. Heeger
Institute for Polymers and Organic Solids, University of California, Santa Barbara, Santa Barbara, California 93106, USA
(Received 14 February 2003; published 6 November 2003)

Excitation-density- and probe-wavelength-dependent pump-probe measurements are used to characterize the excited-state dynamics in pristine polyfluorene. At high excitation densities, a secondary excitation is created at times delayed from the initial formation of excitons. The spectrum of the intermediate state has been characterized by probe-wavelength-dependent measurements. We interpret the results in terms of the generation of charge-separated pairs via a two-step exciton-exciton annihilation process.

DOI: 10.1103/PhysRevB.68.174303 PACS number(s): 78.47.+p, 78.66.Qn, 78.20.−e, 71.35.−y

I. INTRODUCTION

Semiconducting polymers have emerged as materials with interesting optical and electrical properties and promising applications, including light-emitting diodes, lasers, field-effect transistors, solar cells, etc.[1,2] Although extensive research has been carried out with the goal of understanding the photophysics of this class of materials, the nature of the elementary excitations in different semiconducting polymers remains controversial: neutral excitons or charge separated pairs? Debate has focused on the charge generation mechanism:[3] Are charges generated as primary excitations or via a secondary process involving exciton dissociation?

For polymers with PPV backbone structure, transient photoconductivity and ultrafast pump-probe measurements of the photoinduced infrared-active vibrational (IRAV) mode absorption[3–7] demonstrated that the exciton binding energy is less than 0.1 eV. Because of the small exciton binding energy, both neutral excitons and charge-separated pairs are within 100 fs following direct π-π^* photoexcitation in the PPV's; e.g., the branching ratio for charge generation was determined to be ~10% in MEH-PPV.[5–7]

The soluble polyfluorene derivatives—for example, poly(9,9-dioctylfluorene) (PFO)—are high efficiency blue-emitting materials.[8] The polyfluorenes and related copolymers are the only known family of conjugated polymers that emit colors spanning the entire range of visible wavelengths. There is, however, limited information available on the photophysical properties of the polyfluorenes. In a previous publication,[9] we reported the results of a time-resolved study of the excited-state dynamics of pristine polyfluorene and the photoinduced electron transfer reaction from PFO to C_{60}. The results implied that at low excitation densities neutral excitons are the primary photogenerated species in PFO. We report here that at high excitation densities, the pump-probe signals show significantly different decay profiles and striking probe wavelength dependences. The generation of a secondary excitation (intermediate state) via exciton-exciton annihilation and its subsequent decay are directly observed. The spectrum of the intermediate state has been characterized by probe-wavelength-dependent measurements. We interpret the results in terms of the generation of charge-separated pairs via the following two-step exciton-exciton annihilation process:

$$E^* + E^* \rightarrow E^{**} \rightarrow (1-\eta)(E^* + Q) + \eta(p^- + p^+), \quad (1)$$

where E^* represents an exciton, E^{**} represents a higher-energy excited state, Q is the heat generated during radiationless decay back to the single-exciton state, and η is the fraction of the E^*-E^* annihilation events that yield separated charged polaron pairs ($p^- + p^+$).

II. EXPERIMENTS

The ultrafast pump-probe instrumentation has been described in detail elsewhere.[9] Briefly, femtosecond pulses with a repetition rate of 1 kHz were derived from a Spectra-Physics amplified Ti:sapphire system. The 400-nm pump beam (generated by frequency doubling of the 800-nm output from the amplifier) was focused onto the sample with a beam size of ~500 μm. The probe beam, a white light continuum generated from self-phase modulation in a 1-mm sapphire plate, was focused onto the same spot, but with a smaller size (~100 μm) to make certain that only the photoexcited region was probed. The delay between the pump and probe pulses was varied by a computer-controlled translation stage. The signal was detected using a silicon photodiode and a lock-in amplifier after passing through an Oriel tunable bandpass filter (400–700 nm) or interference filters to select the detection wavelength.

The poly(9,9-dioctylfluorene) sample was purchased from American Dye Source, Inc. and carefully characterized for purity. The films were prepared by spin-casting onto quartz substrates from chloroform solution (10 mg/ml), with an optical density of ~1.2 at the absorption maximum (~384 nm). The PFO emission spectrum spans from 400 to 500 nm with peaks at ~418 and ~435 nm. Thus the emission was that of pure PFO with no sign of the energy-shifted peak often observed in the polyfluorenes.[10] The films were prepared and handled in a controlled atmosphere glove box filled with nitrogen and were loaded into a vacuum chamber which was kept under dynamic vacuum ($<10^{-5}$ mbar) during the experiment.

III. RESULTS AND DISCUSSION

A. Excitation density dependence at 480 nm probe wavelength

Excitation-density-dependent time-resolved experiments have been reported for a number of semiconducting

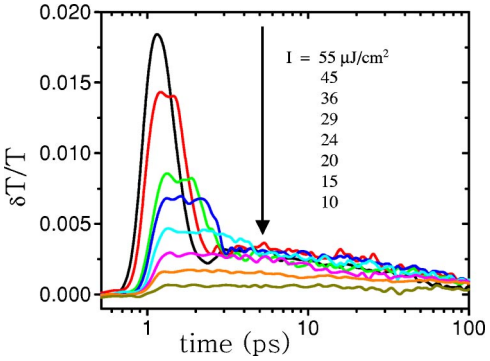

FIG. 1. (Color online) Excitation density dependent pump-probe data obtained from a pristine polyfluorene film with probe wavelength at 480 nm. Time zero was shifted to 1.0 ps for the convenience of presenting the data on a semilog plot.

polymers.[11–16] Higher excitation density usually results in an additional ultrafast decay channel (bimolecular decay), the importance of which diminishes as the excitation density decreases.

Figure 1 shows the excitation-intensity-dependent pump-probe results obtained from PFO with the probe wavelength at 480 nm. At this wavelength, stimulated emission dominates the signal. As the excitation density increases, an additional fast component appears. The amplitude of the fast component is enhanced with even faster decay at higher excitation densities. Note, however, that above a well-defined pump power threshold, the signal level becomes saturated (at delay times >3 ps), and no further increase was observed with increasing excitation density. When the excitation density is high enough, a nonmonotonic time dependence, a ''dip,'' is observed in the time-resolved signal. This dip behavior at high excitation densities has not been previously reported.

For a bimolecular process, the exciton decay rate $d[E^*]/dt$ would be proportional to $[E^*][E^*]$. Thus high excitation densities typically cause a faster signal decay. Assuming that the initial fast decay at high excitation densities results from exciton-exciton annihilation (EEA), the nonmonotonic time dependence could arise from exciton dissociation (for example, to charged pairs or to higher-energy excited states) followed by exciton regeneration. However, it is also possible that there is a negative contribution to the signal from the absorption of an intermediate state generated by the exciton-exciton annihilation. If such a secondary excitation is generated, measurements of the probe wavelength dependence can be used to characterize the spectroscopy of the new species.

B. Probe-wavelength-dependent results at high excitation density

The photoinduced spectra of the neutral exciton, obtained from the transient spectra after photoexcitation at low excitation density (~ 10 μJ/cm^2), were reported earlier.[9] A transition from stimulated emission to photoinduced absorption is observed as the wavelength is shifted to the red with an isosbestic point at 515 nm. Therefore, measurements carried out with probe wavelength near 515 nm minimize the neutral exciton contribution and thus enhance the relative contribution from any transient absorption that arises from an intermediate state at higher pump power.

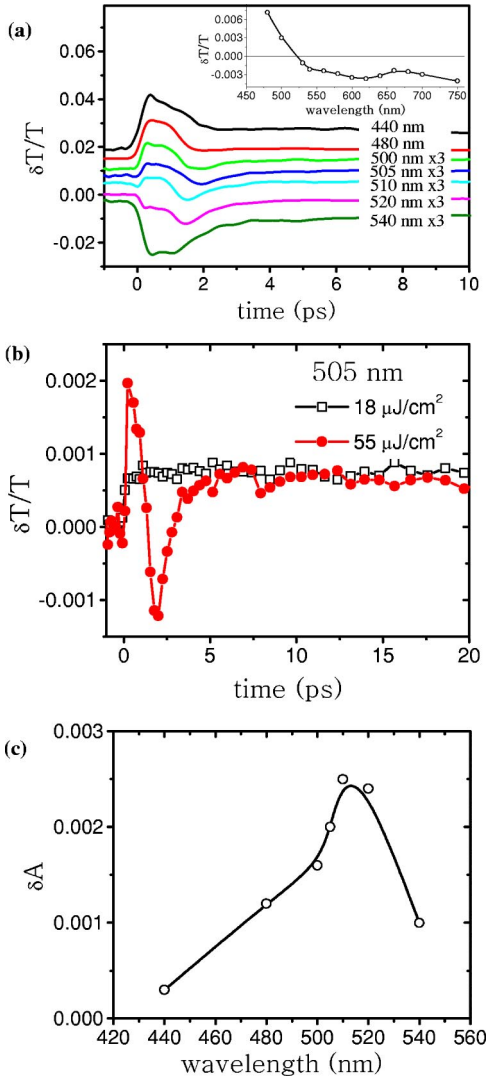

FIG. 2. (Color online) (a) Probe-wavelength-dependent pump-probe data under high excitation density (~ 55 μJ/cm^2). The zero levels for the different probe wavelengths were shifted and the signals rescaled for convenience of presentation. The scaling factors are indicated on the right. The inset is the excited state spectrum (at 0.5 ps delay time) of the pristine PFO film at low excitation density (~ 10 μJ/cm^2). (b) The pump-probe signals (not normalized) obtained at 505 nm probe wavelength at low (18 μJ/cm^2) and high (55 μJ/cm^2) pump intensities are directly compared. (c) Absorption spectrum of the intermediate excited state as reconstructed from the data in (a).

At low excitation densities generated by pumping at 400 nm, the decay profile of the pump-probe signal shows little dependence on the probe wavelength.[9] The situation is quite different at higher excitation densities. As shown in Fig. 2(a), there is a striking probe wavelength dependence when pumped at ~ 55 μJ/cm^2. The dip observed at 480 nm becomes more apparent as the probe wavelength is shifted to

the red; at 505 nm, the signal even changes sign during the decay. When the probe wavelength is further redshifted, a double-peak profile is observed (e.g., at 540 nm). The pump-probe signals at 505 nm (not normalized) obtained at low (18 μJ/cm^2) and high (55 μJ/cm^2) pump intensities are directly compared in Fig. 2(b).

The fact that the signal at 505 nm changes sign at longer delay times at high excitation densities confirms the generation of an intermediate state. The different relative contributions from the exciton (sum of stimulated emission and photoinduced absorption) and the intermediate state (photoinduced absorption) are responsible for the observed wavelength dependence. At short wavelengths, the contribution from the exciton is dominated by stimulated emission,[9] and the overall $\delta T/T$ signal is positive. As the probe wavelength is redshifted from 480 to 510 nm, the net positive signal from the exciton approaches zero at the isosbestic point, and the contribution from the absorption of the intermediate state becomes more apparent and even dominant at intermediate delay times where the nonmonotonic transient signal even changes sign. At 520 nm and longer wavelengths, the net contribution from the exciton is dominated by the photoinduced absorption.[9] The initial small negative shoulder at 520 nm results from the photoinduced absorption contribution from the exciton. The subsequent EEA causes the signal to decay, on the one hand, while the transient absorption of the EEA-generated excitation causes the signal to go even more negative, resulting in the two negative peaks in the decay profiles (see Fig. 2). At 540 nm, the relative amplitude of the two peaks is reversed since the photoinduced absorption from the exciton increases and becomes dominant again.

The probe-wavelength-dependent results unambiguously support the existence of an additional contribution from an EEA-generated species at high excitation densities. The absorption spectrum of this transient species can be reconstructed from the data of Fig. 2(a), as shown in Fig. 2(c). This intermediate-state absorption is located on the long-wavelength side with respect to the ground-state absorption spectrum and overlaps significantly with the spectral features of the charge-separated pairs and neutral exciton.[9] The intermediate-state absorption at even longer wavelengths is quite difficult to determine because of the strong photoinduced absorption of the neutral exciton and appears as a barely seen shoulder in the signal decay.

C. Excitation density dependence at 515 nm

It is clearly of interest to inspect the excitation density dependence of the pump-probe signal with the probe wavelength at the isobestic point where the positive stimulated emission and negative photoinduced absorption from the exciton nearly cancel. Because of this cancellation, the signal at 515 nm is dominated by the contribution from the EEA-generated species. As shown in Fig. 3, a delayed transient absorption signal is observed at high excitation densities; the amplitude increases superlinearly with the pump density. Consistent with the 480-nm data, the rise of this transient absorption moves toward earlier times as the excitation density increases. The excitation density for the onset of the transient absorption from the intermediate state (515-nm data) is coincident with the onset of the initial ultrafast decay in the stimulated emission signal (480-nm data).

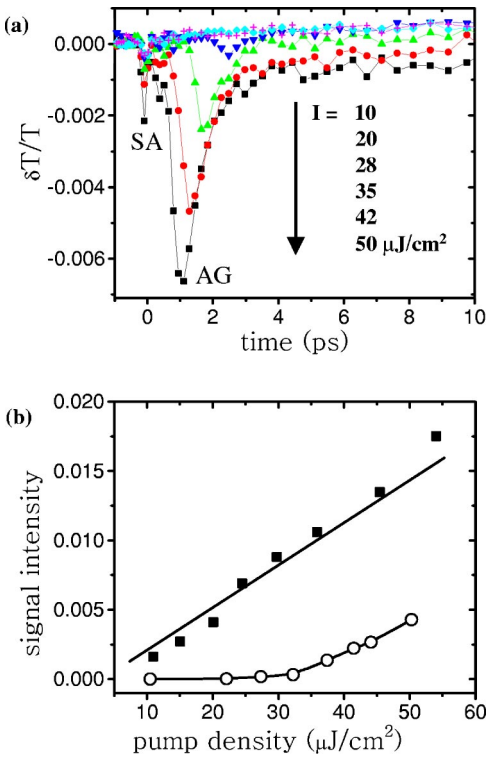

FIG. 3. (Color online) (a) Excitation-density-dependent pump-probe data obtained from a pristine polyfluorene film with probe wavelength at 515 nm. The small negative peak around time zero is labeled as "SA" (sequential absorption) and the delayed one is labeled as "AG" (annihilation generated). (b) The excitation-density-dependent signal levels at 480 nm (solid squares) and 515 nm (open circles).

We note that the decay (disappearance) of the secondary excitation shows a dependence on the excitation density that is different from its generation (the rise in the signal). Whereas the generation is very sensitive to the excitation density, the decay is insensitive. These results suggest that the generation of the secondary excitation is a high-order process, while its decay is a first-order process. The decay can be fit with two exponential components: 0.6 ± 0.1 ps (approximately 90%) and 10 ± 2 ps (approximately 10%).

The creation of the exciton and secondary excitation can be approximately represented by the signal levels at 480 and 515 nm, respectively. Their excitation density dependences are shown in Fig. 3(b). The exciton density varies approximately linearly (within error) with the pump intensity, while the density of the secondary species is not observed at low pump intensities and displays a superlinear increase with increasing pump power. The slight deviation of intensity dependence of the 480-nm signal from linearity suggests that amplified stimulated emission also begins to contribute to the 480-nm signal level at high excitation densities. The excitation dependence of the signal at 515 nm can be fit with a quadratic function, suggesting a bimolecular exciton-exciton annihilation process, although the limited number of points

and the limited resolution do not exclude the possibility of an even higher-order process. In summary, the excitation-density-dependent signals at 480 and 515 nm provide confirming evidence of the generation of a secondary excitation that is generated via exciton-exciton annihilation.

D. Nature of the secondary species generated via exciton-exciton annihilation

The creation of charge-separated pairs through exciton-exciton annihilation is well known in organic semiconductors.[17] In the study of polysilanes, Kepler and Soos[18] proposed the two-step process shown in Eq. (1). As described in Eq. (1), a higher-energy excited state E^{**} is generated via exciton-exciton annihilation. The decay of E^{**} branches into at least two paths: one toward the singlet exciton and the other toward the charge-separated pair. In a general sense, this model is consistent with the data.

It is tempting to identify the time-delayed excitation (the dip) as charge-separated electron-hole pairs or, more specifically, charged polaron pairs. However, previous studies have shown that the lifetimes of charge-separated pairs in PFO and other semiconducting polymers are generally much longer than the lifetimes of the intermediate state observed here.[12,14,16,19–21]

The dynamical behavior of this intermediate state is similar to that reported for a higher excited state in *m*-LPPP, which is prepared by utilization of two sequential pump pulses.[21] In *m*-LPPP, the decay of the higher-energy excited-state decay is biexponential with time scales similar to those obtained in our experiment. The higher excited state was believed to involve branching into at least two paths: one toward the singlet exciton and the other toward the charge-separated pair.[21] Charge carrier generation involving a higher-energy excited state has also been proposed by Frolov *et al.*,[20] Silva *et al.*[19] and Klimov *et al.*[16,22] In their experiments, the higher excited state was generated by sequential absorption within one pump pulse or, purposely, by utilization of two sequential pump pulses.

Evidence of the formation charge-separated polaron pairs is shown in the data in Fig. 3(a), where the signal level at 10 ps delay is observed to shift from positive to negative as the excitation density increases. The rise of the 515-nm signal at low excitation density to positive values at longer delay times can be understood as resulting from the onset of the Stokes shift;[23] i.e., the fluorescence or stimulated emission spectra usually shift to the red in time due to geometric relaxation and excitation migration from short conjugated segments to long conjugated segments. The negative transient absorption at high excitation densities persists to times as long as 100 ps (we have not been able to identify a specific time constant for this long-lived signal as a result of the limited signal-noise ratio). We attribute this slowly decaying contribution to photoinduced absorption by charged polaron pairs.

Similar studies of PFO/C_{60} blends in the high-pump-fluence range showed no dependence of the decay profiles on the excitation density (data not shown here). Therefore, the charge generation process via EEA is not sufficiently fast to compete with the charge transfer process from PFO to the fullerene molecules. This is consistent with the charge carrier pair being created on a relatively slow time scale ($\sim$10 ps) via dissociation of the higher excited state.

In our experiments, the higher-energy excited state (E^{**}) is created through exciton-exciton annihilation [e.g., via the mechanism of Eq. (1)], instead of through sequential excitation. Although sequential pumping within the pulse duration is also likely contribute to generation of the higher-energy excited state [the small negative peak around time zero observed in the 515-nm data obtained at high excitation densities in Fig. 3(a) and the double-peak structure before the dip in the 480-nm data in Fig. 1 might result from this effect], it is not responsible for the time-delayed dip (480-nm data) or the new transient absorption (480- and 515-nm data). The delay time is pump fluence dependent and varies from 1 ps to several picoseconds, much longer than the pulse duration. The fact that both the amplitude and decay time constant of the stimulated emission at 480 nm and the rise of the delayed nonlinear transient absorption signal at 515 nm are pump power dependent and the coincidence of their time scales at the same excitation densities support the argument that exciton-exciton annihilation is responsible for the generation of higher-energy excited states and the subsequent charge separation.

Our conclusion agrees with the speculation by Denton *et al.*[14] based on photophysical modeling of the different SE and PA dynamics. Here we have directly observed the transient absorption associated with E^{**} and its subsequent decay and have characterized the spectrum of this intermediate state. The relative contribution of the two charge-generation mechanisms—sequential absorption (SA) and annihilation generated (AG)—can be estimated from the two peaks in Fig. 3(a) (labeled as ''SA'' and ''AG''), which implies that exciton-exciton annihilation is the dominant mechanism.

Additional studies are required to confirm the nature of the EEA-generated secondary product and to verify the proposed charge generation mechanism (for example, measurements of the photoinduced IRAV absorption). It is unclear whether the intermediate state is a biexcition or a more localized higher excited state of a single chromophore. Even though its absorption spectrum is consistent with the conventional description of biexciton[24]—i.e., on the long-wavelength side of the original chromophore absorption—its lifetime is significantly shorter than the reported biexciton lifetime in nanocrystalline semiconductors and conjugated oligomers.[16,24]

IV. SUMMARY

The results of time-resolved measurements of exciton-exciton annihilation in pristine polyfluorene film are reported. The excitation-density-dependent and probe-wavelength-dependent data obtained at high excitation densities unambiguously establish the correlation between the exciton-exciton annihilation and time-delayed generation of an intermediate state—i.e., a higher-energy intermediate state generated via exciton-exciton annihilation. The absorption spectrum of this intermediate state is located on the

long-wavelength side with respect to the ground-state absorption spectrum and overlaps significantly with the spectral features of the charge-separated pairs and the neutral exciton.

The higher-energy intermediate state subsequently decays (nonradiatively) either back to the singly excited state or by generation of long-lived charge-separated polaron pairs. Although sequential absorption within the pump pulse can contribute to the generation of such doubly excited states and the subsequent charge separation, our results show that exciton-exciton annihilation is the dominant mechanism.

ACKNOWLEDGMENTS

This work was funded by the National Science Foundation (NSF) under Grant No. NSF-DMR 0096820, and by support from the Air Force of Scientific Research (Grant No. AFOSR F49620-02-1-0127, Charles Lee, Program Officer). We thank Wanli Ma for his help in the preparation of the films studied in the experiments and Dr. Steven Xiao (American Dye Source, Inc.) and Dr. Xiong Gong for discussions of the polymer sample.

*Corresponding author. Electronic address: moses@ipos.ucsb.edu

[1] A. J. Heeger, Rev. Mod. Phys. **73**, 681 (2001).

[2] M. D. McGehee, E. K. Miller, D. Moses, and A. J. Heeger, in *Advances in Synthetic Metals: Twenty Years of Progress in Science and Technology*, edited by S. Lefrant, P. Bernier, and G. Bidan (Elsevier, Amsterdam, 1999), p. 98.

[3] N. S. Sariciftci, in *Primary Photoexcitations in Conjugated Polymers: Molecular Excitation versus Semiconductor Band Model*, edited by N. S. Sariciftci (World Scientific, Singapore, 1997).

[4] D. Moses, J. Wang, A. J. Heeger, N. Kirova, and S. Brazovski, Proc. Natl. Acad. Sci. U.S.A. **98**, 13 496 (2001).

[5] P. B. Miranda, D. Moses, and A. J. Heeger, Phys. Rev. B **64**, 1201 (2001).

[6] D. Moses, A. Dogariu, and A. J. Heeger, Chem. Phys. Lett. **316**, 356 (2000).

[7] D. Moses, A. Dogariu, and A. J. Heeger, Phys. Rev. B **61**, 9373 (2000).

[8] M. Leclerc, J. Polym. Sci., Part A: Polym. Chem. **39**, 2867 (2001).

[9] Q.-H. Xu, D. Moses, and A. J. Heeger, Phys. Rev. B **67**, 245417 (2003).

[10] X. Gong, P. K. Iyer, D. Moses, G. C. Bazan, A. J. Heeger, and S. S. Xiao, Adv. Funct. Mater. **13**, 325 (2003).

[11] M. A. Stevens, C. Silva, D. M. Russell, and R. H. Friend, Phys. Rev. B **63**, 5213 (2001).

[12] B. Kraabel, V. I. Klimov, R. Kohlman, S. Xu, H. L. Wang, and D. W. McBranch, Phys. Rev. B **61**, 8501 (2000).

[13] D. Vacar, A. Dogariu, and A. J. Heeger, Adv. Mater. (Weinheim, Ger.) **10**, 669 (1998).

[14] G. J. Denton, N. Tessler, M. A. Stevens, and R. H. Friend, Synth. Met. **102**, 1008 (1999).

[15] C. Silva, M. A. Stevens, D. M. Russell, S. Setayesh, K. Mullen, and R. H. Friend, Synth. Met. **116**, 9 (2001).

[16] V. I. Klimov, D. W. McBranch, N. Barashkov, and J. Ferraris, Phys. Rev. B **58**, 7654 (1998).

[17] M. Pope and C. E. Swenberg, *Electronic Processes in Organic Crystals and Polymers* (Oxford University Press, New York, 1999).

[18] R. G. Kepler and Z. G. Soos, in *Primary Photoexcitations in Conjugated Polymers: Molecular Excitation versus Semiconductor Band Model*, edited by N. S. Sariciftci (World Scientific, Singapore, 1997), p. 363.

[19] C. Silva, A. S. Dhoot, D. M. Russell, M. A. Stevens, A. C. Arias, J. D. MacKenzie, N. C. Greenham, R. H. Friend, S. Setayesh, and K. Mullen, Phys. Rev. B **64**, 125211 (2001).

[20] S. V. Frolov, Z. Bao, M. Wohlgenannt, and Z. V. Vardeny, Synth. Met. **116**, 5 (2001).

[21] C. Gadermaier, G. Cerullo, G Sansone, G. Leising, U. Scherf, and G. Lanzani, Phys. Rev. Lett. **89**, 117402 (2002).

[22] V. I. Klimov, D. W. McBranch, N. N. Barashkov, and J. P. Ferraris, Chem. Phys. Lett. **277**, 109 (1997).

[23] J. L. Bredas, J. Cornil, and A. J. Heeger, Adv. Mater. (Weinheim, Ger.) **8**, 447 (1996).

[24] S. V. Gaponenko, *Optical Properties of Semiconductor Nanocrystals* (Cambridge University Press, New York, 1998).